

Searching for the Slater transition in the pyrochlore $\text{Cd}_2\text{Os}_2\text{O}_7$ with infrared spectroscopy

W. J. Padilla

Department of Physics, University of California San Diego, La Jolla, California 92093-0319

D. Mandrus

Solid State Division, Oak Ridge National Laboratory, Oak Ridge, Tennessee 37831

D. N. Basov

Department of Physics, University of California San Diego, La Jolla, California 92093-0319

(Received 18 January 2002; published 31 July 2002)

Infrared reflectance measurements were made on the single crystal pyrochlore $\text{Cd}_2\text{Os}_2\text{O}_7$ in order to examine the transformations of the electronic structure and crystal lattice across the boundary of the metal-insulator transition (MIT) at $T_{MIT}=226$ K. All predicted IR active phonons are observed in the conductivity over all temperatures and the oscillator strength is found to be temperature independent. These results indicate that charge ordering plays only a minor role in the MIT and that the transition is strictly electronic in nature. The conductivity shows the clear opening of a gap with $2\Delta=5.2k_B T_{MIT}$. The gap opens continuously, with a temperature dependence similar to that of Bardeen-Cooper-Schrieffer (BCS) superconductors, and the gap edge having a distinct $\sigma(\omega)\sim\omega^{1/2}$ dependence. All of these observables support the suggestion of a Slater transition in $\text{Cd}_2\text{Os}_2\text{O}_7$.

DOI: 10.1103/PhysRevB.66.035120

PACS number(s): 78.30.-j

Mott's classic paper,¹ published over half a century ago, has triggered extensive research on correlated electron systems which undergo a MIT. Both Mott and Hubbard² have suggested that for systems at half filling, the Coulomb repulsion between electrons could split the band, thus yielding an insulator. Alternatively, Slater in 1951 suggested that antiferromagnetic order alone could produce an insulator by a doubling of the magnetic unit cell.³ While there are numerous examples of Slater/spin-density-wave (SDW) insulators in the realm of one-dimensional (1D) conductors,^{4,5} the experimental situation at higher dimensions is less clear. Impossibility of the Slater state in the 2D regime has been recently argued based on dynamical cluster approximation calculations.⁶ For 3D solids, spin ordering alone usually generates an energy gap corrupting only a fraction of the Fermi surface so that metallic conductivity persists.⁷ In this context, the metal-insulator transition in the 3D pyrochlore $\text{Cd}_2\text{Os}_2\text{O}_7$ is exceptionally intriguing since transport and magnetic properties across the MIT boundary appear to be in accord with the Slater mechanism.⁸ In this paper we report on our spectroscopic studies of the MIT in $\text{Cd}_2\text{Os}_2\text{O}_7$. Our analysis of the infrared data reveals that the transition into the insulating state is driven solely by the electronic interactions without significant involvement of the crystal lattice. We discuss new facets of the spin-driven insulating state in a 3D material.

The pyrochlore $\text{Cd}_2\text{Os}_2\text{O}_7$ was first characterized by Sleight *et al.*⁹ The metal-insulator transition in the resistivity has been found to occur at the same temperature, ≈ 226 K, as the antiferromagnetic transition in susceptibility measurements. No evidence of concurrent structural changes were detected through x-ray diffraction (XRD) analysis. Thorough examination of transport and magnetism in $\text{Cd}_2\text{Os}_2\text{O}_7$ has been recently reported by Mandrus *et al.*⁸ with a Slater picture delivering a coherent interpretation of all experimental

data. This particular mechanism in $\text{Cd}_2\text{Os}_2\text{O}_7$ may be favored by the fact that Os^{5+} is in the $5d^3$ configuration so that the t_{2g} band is near half filling.

The Slater transition is characterized by several hallmarks in the frequency domain which so far remained unexplored in $\text{Cd}_2\text{Os}_2\text{O}_7$. Among them are the specific temperature dependence of the energy gap and the frequency dependence of the dissipative response at energies above the gap edge that are distinct from the Mott-Hubbard case.¹⁰ Also, the analysis of the IR active phonon modes allows one to verify if a development of charge ordering is concomitant with spin ordering. Despite the fact that IR spectroscopy is ideally suited for directly studying the nature of the MIT in solids, the extremely small size of $\text{Cd}_2\text{Os}_2\text{O}_7$ single crystals so far has rendered these measurements impossible. Spectroscopic tools available in our lab at UCSD are tailored for investigations of microcrystals,¹¹ allowing us to fill voids in the experimental picture of the insulating state in $\text{Cd}_2\text{Os}_2\text{O}_7$.

The near-normal reflectance $R(\omega)$ of $\text{Cd}_2\text{Os}_2\text{O}_7$ was measured from 40 cm^{-1} to $14\,000\text{ cm}^{-1}$ using a Fourier transform spectrometer and from $12\,000\text{ cm}^{-1}$ to $35\,000\text{ cm}^{-1}$ using a grating monochromator. A test involving polarized light displayed no signs of anisotropy, thus unpolarized radiation was used for a detailed study of the temperature dependence. Samples were coated *in situ* with gold or aluminum, and spectra measured from the coated surface were used as a reference. This method, discussed previously in detail,¹² allows one to reliably obtain the absolute value of the reflectance by minimizing the errors associated with non-specular reflection and small sample size. We inferred the complex conductivity $\sigma_1(\omega)+i\sigma_2(\omega)$ by use of Kramers-Kronig (KK) analysis after extrapolating data to $\omega\rightarrow 0$ and $\omega\rightarrow\infty$. Various low-frequency extrapolations (Drude, Hagen-Rubens) were used; however the data did not significantly depend on the particular method of low- ω extrapolation.

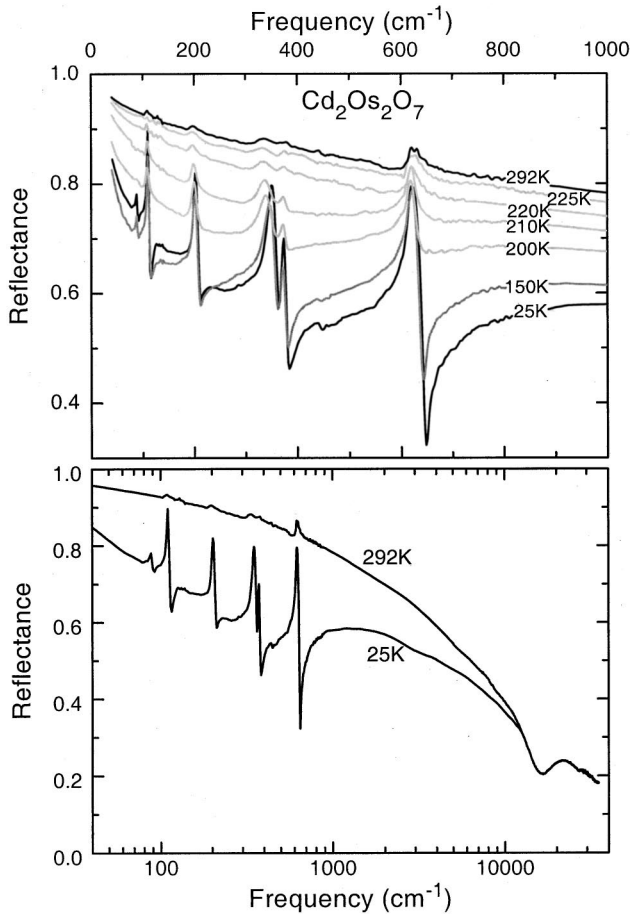


FIG. 1. Reflectance of single crystal $\text{Cd}_2\text{Os}_2\text{O}_7$ at various temperatures from 40 cm^{-1} to 1000 cm^{-1} . The entire energy range characterized is shown in the bottom panel for room temperature and 25 K on a log scale.

tion. We employed the usual ω^{-4} dependence for the high-energy extension of the data.¹³

The top panel of Fig. 1 shows the infrared reflectance taken between 25 K and room temperature from an unpolished facet of $\text{Cd}_2\text{Os}_2\text{O}_7$ crystal with dimensions less than $0.5 \times 0.7 \text{ mm}^2$. The reflectance at room temperature is high and is metallic in nature. $R(\omega)$ decreases with decreasing temperature in the infrared region. Although the reflectance decreases monotonically, it changes little near room temperature and at low temperatures. Depression of $R(\omega)$ is most significant in the vicinity of the MIT: between 225 K and 150 K. The absolute value of the reflectance for the 80 K data is, within experimental accuracy, equivalent to that at 25 K. As temperature is lowered the free electron screening is gradually reduced unveiling several strong phonons in the infrared region. Notably, all phonons are still visible in the room temperature data. In the bottom panel of Fig. 1 we plot the reflectance over the entire range characterized for room temperature and 25 K.

Figure 2 shows the real part of the conductivity $\sigma_1(\omega)$ at different temperatures. The room temperature spectrum can be adequately described with a simple Drude model $\sigma_1(\omega) = \sigma_0 / (1 + \omega^2 \tau^2)$ at least for $\omega < 1000 \text{ cm}^{-1}$ where σ_0 is the

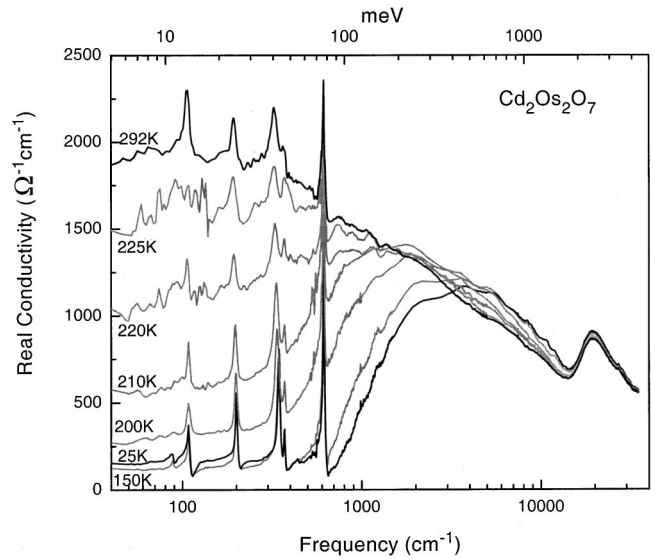


FIG. 2. Real part of the optical conductivity as obtained by Kramers-Kronig analysis on a log scale. A gap can be seen to develop continuously as the temperature is reduced. The reduction in spectral weight occurring in the infrared region is compensated by a shift to higher energies.

DC conductivity and τ is the relaxation time. This behavior is followed by a somewhat slower decrease than that prescribed by the Drude form, and an interband feature at 22 000 cm^{-1} . Several strong phonons are visible in the IR region. As the temperature is lowered, one witnesses the continuous opening of a gap with a drastic reduction of $\sigma_1(\omega)$ in the infrared. In the 25 K spectrum the intragap conductivity is frequency independent (apart from the sharp phonon peaks). At ω above the gap edge the spectrum reveals the $\omega^{1/2}$ dependence expected for a Slater transition.^{10,14} An intersection between the two segments at 818 cm^{-1} can be chosen as a quantitative measure of the energy gap 2Δ . The $\omega^{1/2}$ behavior can be recognized at higher temperatures as well. In the latter spectra (Fig. 3) the intragap region is best described with a linear dependence. The temperature dependence of the intersection between the $\sigma_1(\omega) \propto \omega$ and $\sigma_1(\omega) \propto \omega^{1/2}$ regions is plotted in the inset of Fig. 3.

It is instructive to characterize the development of the energy gap in $\text{Cd}_2\text{Os}_2\text{O}_7$ through the spectra of the effective spectral weight $N_{eff}(\omega) = (120/\pi) \int_0^\omega \sigma_1(\omega') d\omega'$. The magnitude of $N_{eff}(\omega)$ depicted in Fig. 4, is proportional to the number of carriers participating in the optical absorption up to a cutoff frequency ω , and has the dimension of frequency squared. The significant reduction in spectral weight occurring in the intragap region is transferred to the energy region above 3Δ . Interestingly, the spectral weight does not become completely exhausted until 16 000 cm^{-1} , implying that the energy range as broad as $40\Delta \approx 104 k_B T_{MIT}$ is involved in the metal-insulator transition.

Important insights into the origin of the insulating state in $\text{Cd}_2\text{Os}_2\text{O}_7$ may be reached through the analysis of the phonon spectra. The pyrochlore structure belongs to the space group $Fd\bar{3}m$ and reveals seven IR active modes.^{15,16} We observe phonon peaks at 86 cm^{-1} , 108 cm^{-1} , 200 cm^{-1} ,

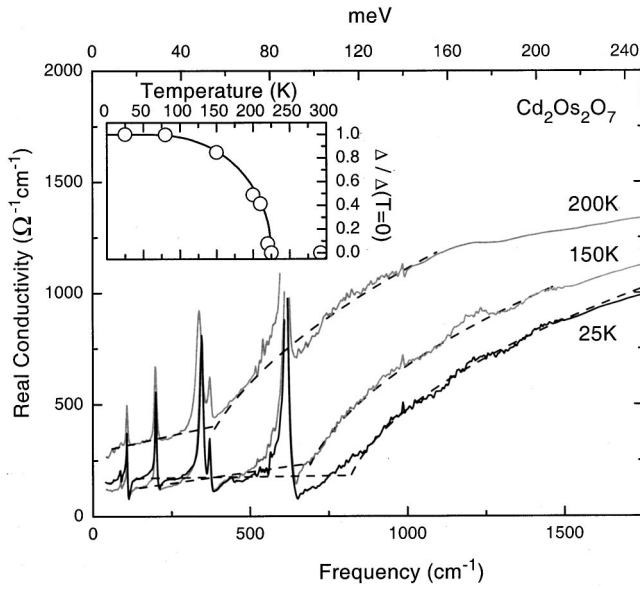


FIG. 3. Infrared region of the real conductivity at $T < T_{MIT}$. The expected theoretical frequency dependence of the gap edge [$\sigma_1(\omega) \propto \omega^{1/2}$] is shown for each temperature as a dashed line. A linear fit for the region below the gap edge is also shown. The intersection of the two fits can be taken as a measure of the energy gap 2Δ . The inset shows the optical energy gap as determined by the method described above (open circles), and the expected theoretical dependence (solid curve).

347 cm^{-1} , 371 cm^{-1} , 440 cm^{-1} , and 615 cm^{-1} in the 25 K spectrum.¹⁷ Both the frequency position and the oscillator strength of all phonons (with the exception of the 347 cm^{-1} resonance) are independent of temperature (bottom panel of Fig. 5). The 347 cm^{-1} mode assigned to the $O_{II}-Os-O_{II}$ bend¹⁵ shows weak hardening at $T < T_{MIT}$. The key outcome

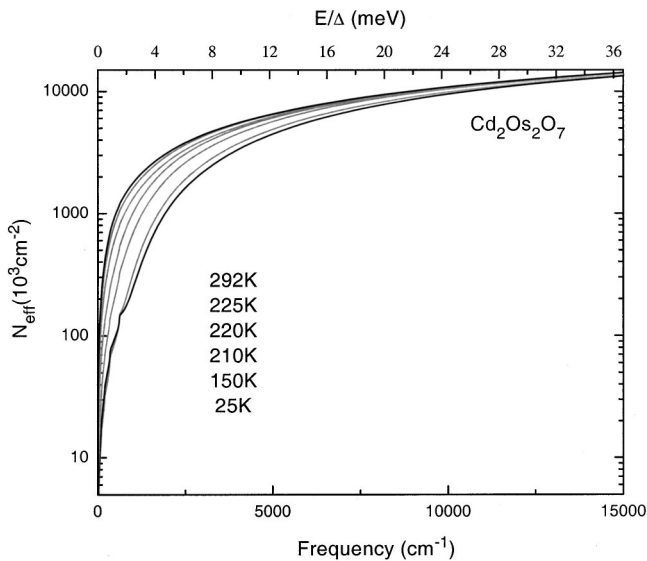


FIG. 4. Effective spectral weight vs cutoff frequency for temperatures as indicated. The top axis is in energy units normalized by the gap energy. The spectral weight can be seen to have significant dependence until about $40\Delta \approx 104k_B T_{MIT}$.

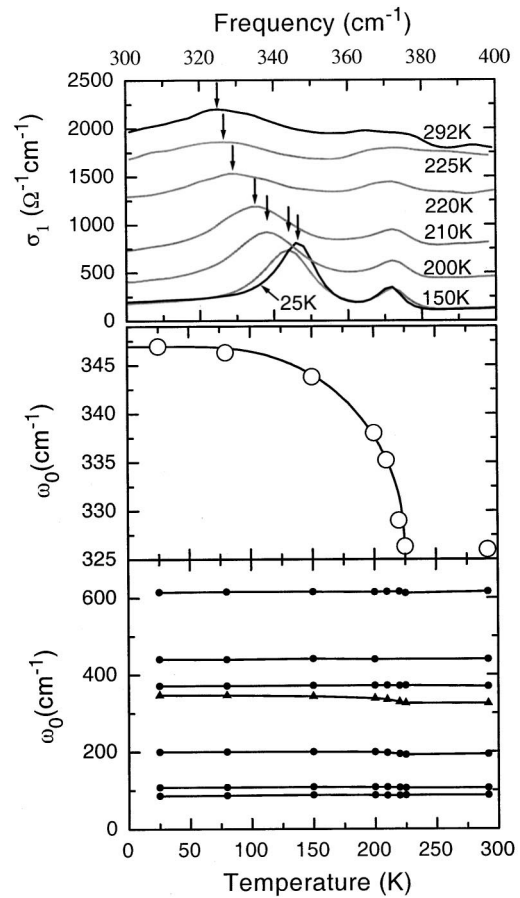


FIG. 5. The top panel shows a detail of the 347 cm^{-1} phonon as observed in the real conductivity, which is seen to harden with decreasing temperature. The middle panel displays the temperature dependence of the 347 cm^{-1} phonon and the BCS gap function is also plotted (solid curve). The bottom panel gives the temperature dependence of all seven phonons.

of the examination of the phonon spectra in Figs. 1 and 2 is that no new phonon modes appear at $T = T_{MIT}$ and the low- T data for $\text{Cd}_2\text{Os}_2\text{O}_7$ displays only the seven modes expected for the ideal pyrochlore structure.

The experimental evidence presented above suggests that the development of the insulating state in $\text{Cd}_2\text{Os}_2\text{O}_7$ occurs without visible signs of charge ordering. Examination of the IR-active phonons has proven to be one of the most sensitive tests for the charge-ordered state. Quite commonly additional lattice modes appear in the phonon spectra, or a dramatic redistribution of the spectral weight between several resonances takes place provided the system reduces its symmetry in the charge-ordered regime.¹⁸ We failed to detect any of these effects. Furthermore, a detailed analysis of the x-ray diffraction data did not produce any indications for structural changes at $T < T_{MIT}$.⁸ These observations allow us to conclude that the metal-insulator transition in $\text{Cd}_2\text{Os}_2\text{O}_7$ is driven solely by electronic processes without noticeable indications for involvement of the lattice. Another important fact pertaining to the nature of the insulating state is the continuous development of the energy gap in the electronic conductivity displayed in Fig. 2, which is consistent with the

Slater picture of the MIT.^{19,20} The second order transition is in accord with earlier specific heat and magnetic susceptibility data.⁸

Further support for the Slater hypothesis in the context of the $\text{Cd}_2\text{Os}_2\text{O}_7$ data is provided by the electronic conductivity. We first note that our data reveal several hallmarks of the BCS electrostatics expected for systems with spin-density waves,⁵ including the ratio of $2\Delta/k_B T_{MIT} \approx 5.1$ (expected in a modified BCS theory that takes into account the scattering of electrons by phonons, as for the canonical SDW chromium)^{21,22} as well as a characteristic decline of the gap value at nonzero temperatures.^{19,20} The general form of the conductivity spectra is also consistent with the BCS picture where type-2 coherence factors lead to an overshoot between the data at $T \ll T_{MIT}$ and $T > T_{MIT}$ at frequencies above the gap. As pointed out above, the behavior of the low- T spectra above the gap edge is adequately described with the $\sigma_1(\omega) \sim \omega^{1/2}$ dependence, as is expected for a Slater transition. This finding is important because the $\omega^{1/2}$ dependence is distinct from the $\omega^{3/2}$ dependence observed in the Hubbard limit.¹⁰

Given the experimental evidence discussed above, the Slater mechanism emerges as a viable model of the MIT in $\text{Cd}_2\text{Os}_2\text{O}_7$. Therefore, this compound may be the first well-documented case of a three-dimensional SDW²³ material,²⁴ subject to further direct verification of the spin structure.²⁵ An unexpected feature of the antiferromagnetically-driven

MIT is a mismatch between the $T_{MIT} \approx 200$ K and the frequency range involved in the redistribution of the spectral weight in the insulating state $\Omega \approx 20\,000$ K. Similar mismatch is commonly found throughout the spectroscopic studies of the so-called pseudogap state in high- T_c superconductors,²⁶ in which antiferromagnetic fluctuations are perceived as a likely cause of the pseudogap state. Finally, it is worth mentioning that other pyrochlore compounds reveal very different properties at the verge of the metal-insulator transition. For instance, the transition to the insulating regime in the closely related $\text{Tl}_2\text{Ru}_2\text{O}_7$ system appears to be of first order, and additionally is accompanied by charge-ordering effects judging from the transformations of the phonon spectra.²⁷ $\text{Cd}_2\text{Os}_2\text{O}_7$ is, to our knowledge, the only transition metal oxide that shows a continuous MIT. Additionally, $\text{Cd}_2\text{Os}_2\text{O}_7$ is the only known material in which Cd is the magnetic element responsible for magnetic ordering, should magnetic order be found. It is yet to be determined what microscopic factors define the peculiar character of the MIT in $\text{Cd}_2\text{Os}_2\text{O}_7$.

Work performed at UCSD was sponsored by the U.S. Department of Energy under Contract No. DE-FG03-00ER45799. Work at Oak Ridge National Laboratory is managed by UT-Battelle, LLC, for the U.S. Department of Energy under Contract No. DE-AC05-00OR22725.

¹N.F. Mott, Proc. Phys. Soc., London, Sect. A **62**, 416 (1949).

²J. Hubbard, Proc. R. Soc. London, Ser. A **276**, 238 (1963).

³J.C. Slater, Phys. Rev. **82**, 538 (1951).

⁴L. Degiorgi, M. Dressel, A. Schwartz, B. Alavi, and G. Gruner, Phys. Rev. Lett. **76**, 3838 (1996); V. Vescoli, L. Degiorgi, M. Dressel, A. Schwartz, W. Henderson, B. Alavi, G. Gruner, J. Brinckmann, and A. Virosztek, Phys. Rev. B **60**, 8019 (1999).

⁵G. Gruner, *Density Waves in Solids* (Perseus Publishing, Massachusetts, 1994).

⁶S. Moukouri, M. Jarrell, Phys. Rev. Lett. **87**, 167010 (2001).

⁷A canonical example of a 3D SDW system is Cr, discussed in detail in E. Fawcett, Rev. Mod. Phys. **60**, 209 (1988).

⁸D. Mandrus, J.R. Thompson, R. Gaal, L. Forro, J.C. Bryan, B.C. Chakoumakos, L.M. Woods, B.C. Sales, R.S. Fishman, and V. Keppens, Phys. Rev. B **63**, 195104 (2001).

⁹A.W. Sleight, J.L. Gillson, J.F. Weiher, and W. Bindloss, Solid State Commun. **14**, 357 (1974).

¹⁰G.A. Thomas, D.H. Rapkine, S.A. Carter, A.J. Millis, T.F. Rosenbaum, P. Metcalf, and J.M. Honig, Phys. Rev. Lett. **73**, 1529 (1994).

¹¹S.V. Dordevic, N.R. Dilley, E.D. Bauer, D.N. Basov, M.B. Maple, L. Degiorgi, Phys. Rev. B **60**, 11321 (1999).

¹²C. Homes, M.A. Reedyk, D.A. Crandels, and T. Timusk, Appl. Opt. **32**, 2976 (1993).

¹³F. Wooten, *Optical Properties of Solids* (Academic Press, New York, 1972).

¹⁴A.J. Millis (private communication).

¹⁵R.A. McCauley, J. Opt. Soc. Am. **63**, 721 (1972).

¹⁶B.A. DeAngelis, R.E. Newham, and W.B. White, Am. Mineral. **57**, 255 (1972).

¹⁷Of these seven phonons, six can easily be resolved in $\sigma_1(\omega)$ shown in Fig. 2, and a small hard-to-see phonon ω_3 located at 440 cm^{-1} can be resolved easiest in Fig. 1 in the lower temperature data sets.

¹⁸E. Buixaderas, S. Kamba, J. Petzelt, M. Savinov, and N.N. Kolpakova, Eur. Phys. J.: Appl. Phys. **19**, 9 (2001).

¹⁹T. Matsubara and Y. Yokota, in Proceedings of the International Conference on Theoretical Physics, Kyoto-Tokyo 1953 (Sci. Council Japan, Tokyo, 1954), p. 693.

²⁰J. Des Cloizeaux, J. Phys. Radium **20**, 606 (1959).

²¹A.S. Barker, B.I. Halperin, and T.M. Rice, Phys. Rev. Lett. **20**, 384 (1968).

²²Strong inelastic scattering has also been suggested as a reason for the larger than expected values of $2\Delta/k_B T_{MIT}$, see for, e.g., Stefan Blawid and Andrew Millis, Phys. Rev. B **62**, 2424 (2000).

²³The MIT in Cd has also been interpreted as due to an excitonic instability, as electronic structure calculations show an isotropic Fermi surface with no nesting features. See D.J. Singh, P. Blaha, K. Schwarz, and J.O. Sofo, Phys. Rev. B **65**, 155109 (2002).

²⁴Although the MIT in the 3D Perovskite-type oxide NdNiO_3 has been attributed to the formation of a SDW, the lattice parameters show an abrupt change at $T < T_{MIT}$. While a depression of the conductivity has been observed in this work, it is difficult to judge on the T -dependence of the gap and on the form of $\sigma_1(\omega)$ across the gap. This as well as the large $2\Delta/k_B T_{MIT} \sim 20$ ratio

- pose problems for a SDW interpretation of the data. See T. Katsufuji, Y. Okimoto, T. Arima, and Y. Tokura, *Phys. Rev. B* **51**, 4830 (1995).
- ²⁵Powder neutron diffraction indicates no long-range magnetic order down to 12 K. This inconsistency with the Slater interpretation may be connected with magnetic frustration inherent in the pyrochlore lattice. See J. Reading and M.T. Weller, *J. Mater. Chem.* **11**, 237 (2001).
- ²⁶D.N. Basov, E.J. Singley, and S.V. Dordevic, *Phys. Rev. B* **65**, 054516 (2002).
- ²⁷J.S. Lee, Y.S. Lee, K.W. Kim, and T.W. Noh, *Phys. Rev. B* **64**, 165108-1 (2001).